COBEM 2023 27TH INTERNATIONAL CONGRESS OF MECHANICAL ENGENEERING

ABCM Brazilian Society of Mechanical Sciences and Engineering
27th ABCM International Congress of Mechanical Engineering
December 04-08, 2023, Florianópolis-SC, Brazil

COB-2023-0457
A Modal Reduction Scheme for the Free Vibration of Strings with Inertially Loaded Boundary

Pedro Menescal Jales
Rubens Gonçalves Salsa Junior
Vinícius Lamas von Sohsten
Universidade Federal do Rio Grande do Norte, Lagoa Nova, 59078-970.
pedro.jales.017@ufrn.edu.br, rubens.salsa@ufrn.br, vinicius.von.059@ufrn.edu.br

Abstract. *In structural engineering, it is essential to minimize computational costs when simulating systems governed by differential equations. Modal reduction techniques are widely employed to achieve this objective without compromising accuracy. These techniques involve excluding higher-order modes that have negligible influence on the system's response. This study proposes a modal reduction scheme designed for the free vibration analysis of a string with fixed-inertially loaded boundaries. Modified orthogonality relationships, considering the boundary conditions, are derived to determine the modal shapes. Through the modal expansion, the original partial differential equation of motion is transformed into a set of independent ordinary differential equations solvable for the modal coordinates. The methodology estimates modal participation factors by analyzing the energy distribution among modal coordinates. The proposed scheme significantly reduces computational expenses by disregarding less significant modes and accuracy of the reduced model is evaluated using absolute and root mean square error expressions. The effectiveness of the modal reduction scheme is demonstrated through three illustrative examples: validating the methodology by exciting a single mode, releasing a linearly stretched string, and plucking the string at its midpoint. This modal reduction approach provides a practical solution for maintaining accuracy while significantly reducing computational costs in simulating the system dynamic behavior.*

Keywords: *modal reduction, modal analysis, strings, orthogonality, modal participation.*

1. INTRODUCTION

A string is a one-dimensional elastic continuum that does not transmit or resist bending moment. The same principle applies to cables when their thickness-to-length ratio is significantly small (Hagedorn and DasGupta, 2007). The vibration of strings and cables is an important field of structural engineering and knowledge of their dynamic behavior is indispensable in designing and optimizing mechanical components, such as suspension bridges, cranes, oil rig risers used in offshore drilling and the belts used in power steering of internal combustion engines.

Strings have stationary motions at certain frequencies known as mode shapes. For the common boundary fixed-fixed conditions, it is well known that these modes satisfy the usual orthogonality relationships. Modal orthogonality is important because it allows the transformation of the partial differential equations of motion into a system of infinitely many independent ordinary differential equations for the modal coordinates. The solution of these equations is used to recover the dynamic behavior of the string through an infinite sum of modal motions, which is not possible to resolve computationally. Hence, it is vital for structural engineers to explore techniques that reduce the degrees of freedom in a system, thereby reducing computational costs while maintaining reasonable accuracy. One prevalent approach to achieve this reduction is known as modal reduction (Genta, 2009), which involves performing the aforementioned modal transformation and selecting a set of mode shapes to form a reduced basis for the approximate solution.

Modal reduction serves several essential purposes. Firstly, for intricate systems with numerous modes, modal reduction provides a simplified model that approximates the original system's behavior, aiding in predictive insights. In structural engineering, this is valuable for analyzing vibrations by identifying critical frequencies and mitigating potential issues through the focus on dominant modes. In addition, this reduction technique is indispensable in control theory, where it facilitates the design of controllers for lower-order models, making them more amenable to analysis and control, thereby aiding practical control system design (Besselink *et al.*, 2013). Finally, it streamlines the analysis of large-scale systems where solving the full model is computationally taxing. Consequently, modal reduction plays a pivotal role in simplifying complex systems, improving their manageability, and enhancing computational efficiency.

This procedure is more evolved in the case of multibody systems, like a string attached to a harmonic oscillator, for example. In these cases the mode shapes do not satisfy the usual orthogonality relationships, so selection of an appropriate modal base is not trivial. For instance, it has been shown that a homogeneous string fixed at both ends and loaded with a finite number of masses possesses symmetric and antisymmetric vibration modes. The symmetric modes have a discontinuous slope at the points where the masses were loaded, whereas the antisymmetric ones have a continuous

slope, with nodes at the positions of the attached masses (Gómez *et al.*, 2007, 2009; Cox *et al.*, 2012; Wenin, 2022; Jung *et al.*, 2021).

Numerous methods have been proposed to construct a modal basis for these types of problem, and they may consist of eigenmodes derived from fully-clamped, partially-clamped, or free-floating structures. Alternatively, experimentally measured modes can also be utilized. One approach was presented by Craig Jr and Bampton (1968), who employs the natural vibration mode shapes of a structure clamped at all interface nodes. However, the use of fully-clamped modes as employed in Craig-Bampton's method often fails to provide an appropriate basis for modal reduction in general multibody systems (Sonneville *et al.*, 2021). On the other hand, Rubin (1975) proposed a method that utilizes the natural vibration mode shapes of a free-floating structure, which appear to be more suitable for flexible multibody systems. Nonetheless, this approach introduces higher complexity in describing the interfaces due to the influence of modal amplitudes on displacements at the interface node. Recent approaches involve projecting the equations onto non-eigenmode-based modes Fehr and Eberhard (2011) or incorporating information about the nonlinear behavior of the structure Haller and Ponsioen (2016).

In this light, the purpose of this work is to report a modal reduction scheme for a homogeneous string in free vibration, clamped at one end and connected to a point mass at the other boundary. A modified orthogonality relationship for the physically excitable modes is derived and used to obtain a system of differential equations for the modal coordinates. Then, the reduced modal basis is formed through the highest modal participation factors, which are estimated using the energy distribution among modal coordinates, as proposed by Salsa Jr. and Ma (2021). The scheme is applied to three different case studies: (i) when only the second mode is excited, (ii) when the string is linearly stretched and released, and (iii) when the string is plucked at the center and released from rest. In all cases, the accuracy of the approximate solution is estimated using the absolute error and a root mean square error. It is shown that the proposed methodology produced accurate approximations using only a few modes. The organization is as follows: the system under investigation and its free vibration characteristics are expounded in Section 2. The modal reduction scheme is explained in Section 3. Applications and results are discussed in Section 4. Concluding remarks are listed in Section 5.

2. SYSTEM MODEL

In this section, the model of the structure under investigation is discussed.

2.1 Equation of Motion

The equation of motion that describes the small transverse motion of uniform strings in free vibration, shown in Fig. 1, may be obtained by applying Newton's second law of motion to an infinitesimal element of the string, resulting in a partial differential equation of the form (O'Reilly, 2017; Meirovitch, 2001)

$$\frac{\partial^2 y}{\partial x^2} = \frac{1}{c^2}\frac{\partial^2 y}{\partial t^2}, \tag{1}$$

with domain $x \in (0, L)$ and $t \geq 0$. Here, $y(x,t)$ represents the transversal displacement from equilibrium at position x and time t, $c = \sqrt{T/\rho}$ is the speed of transverse waves that travel on the string, with T and ρ as constant properties of the string representing the tension and density (mass per unit length), respectively. This equation is complemented by the set of initial conditions

$$y(x, t=0) = \hat{g}(x), \quad \frac{\partial y}{\partial t}(x, t=0) = \hat{h}(x), \tag{2}$$

and boundary conditions

$$y(x=0, t) = 0, \quad T\frac{\partial y}{\partial x}(x=L, t) = -m\frac{\partial^2 y}{\partial t^2}(x=L, t). \tag{3}$$

To simplify the algebra and streamline computational implementation, the displacement and time variables can be nondimensionalized according to

$$u = \frac{x}{L}, \quad v = \frac{y}{L}, \quad \tau = \frac{c}{L}t. \tag{4}$$

In this manner, the equation of motion and associated initial and boundary conditions are rewritten as

$$\frac{\partial^2 v}{\partial u^2} = \frac{\partial^2 v}{\partial \tau^2}, \tag{5}$$

$$v(u, \tau=0) = g(u), \quad \frac{\partial v}{\partial \tau}(u, 0) = h(u), \tag{6}$$

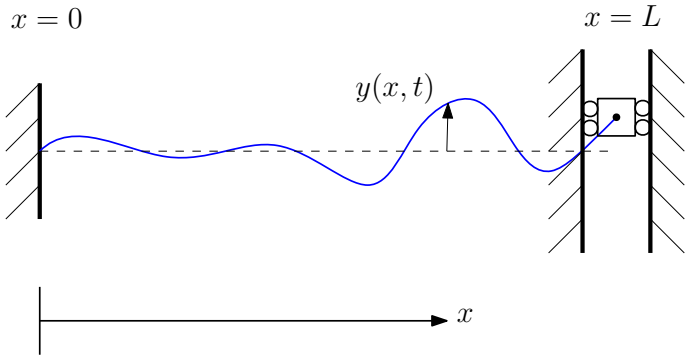

Figure 1. A uniform string of length L in transverse vibration. The string is clamped at $x = 0$ and connected to a particle of mass m at $x = L$.

$$v(u = 0, \tau) = 0, \quad \frac{\partial v}{\partial u}(u = 1, \tau) = -\gamma \frac{\partial^2 v(u = 1, \tau)}{\partial \tau^2}. \tag{7}$$

In the sequence, Eqs. (5)-(7) will be considered, where the nondimensional parameter γ represents the ratio between lumped mass and mass of the string, $\gamma = m/\rho L$.

2.2 Natural Frequencies and Mode Shapes

This inertially-loaded string has been observed to move in stationary wave forms when excited at specific frequencies (Gómez *et al.*, 2007; Mouchet, 2008; Cox *et al.*, 2012; Jung *et al.*, 2021; Wenin, 2022). These frequencies are called natural frequencies and are obtained from the transcendental equation

$$tan(\omega) = \frac{1}{\gamma\omega}. \tag{8}$$

The above equation possesses an infinite number of solutions and can only be solved numerically. The $n-th$ zero ω_n is associated with a stationary solution

$$V_n(u) = sin(\omega_n u) \tag{9}$$

known as normal mode of vibration. There are infinitely many eigenfunctions $V_n(u)$ and they are defined only as far as their shape is concerned, exactly as is the case for eigenvectors of discrete systems. The amplitude of the various modes can be computed only after the initial conditions have been stated.

Due to the nature of the boundary conditions (7), an arbitrary pair of modes V_s and V_r ($s \neq r$) generally does not satisfy the usual orthogonality relationship based on the inner product

$$\langle V_s, V_r \rangle = \int_0^1 V_s V_r du \neq 0. \tag{10}$$

Since orthogonality is important to obtain independent modal equations, this issue can be circumvented by defining a modified inner product

$$\langle\langle a, b \rangle\rangle = \int_0^1 a(u)b(u)du + \gamma a(1)b(1) \tag{11}$$

for any square integrable functions a and b defined on $(0, 1]$ (Boggess and Francis, 2009). With aid of the boundary conditions (7), it can be verified that the eigenfunctions satisfy the modified orthogonality relationship

$$\langle\langle V_s, V_r \rangle\rangle = \int_0^1 V_s(u)V_r(u)du + \gamma V_s(1)V_r(1) = \delta_{sr} = \begin{cases} 1, & s = r \\ 0, & s \neq r \end{cases}. \tag{12}$$

Note that the modes have been normalized in Eq. (12) in such a way that each arbitrary scaling constant C_n in $V_n(u) = C_n sin(\omega_n u)$ is given by

$$C_n = \sqrt{\frac{1}{\int_0^1 V_n^2 du + \gamma V_n^2(1)}}. \tag{13}$$

3. Modal Reduction Scheme

In this section, the modal reduction scheme is explained.

3.1 Modal Coordinates

The mode shapes are orthogonal according to Eq. (12), therefore they are linearly independent and form a basis for the solution space of Eq. (5):

$$v(u,\tau) = \sum_{n=1}^{\infty} V_n p_n(\tau), \tag{14}$$

where $p_n(\tau)$ are the modal coordinates. This is known as modal expansion of the response. Substituting this form into Eq. (5) and using the orthogonality relationship (12), one produces the system of infinitely many independent modal equations

$$\ddot{p}_n + \omega_n p_n = 0, \quad (n = 1, 2, 3, ...) \tag{15}$$

where $\ddot{p}_n = d^2p/d\tau^2$. The general solution of each of these equations is

$$p_n(\tau) = A_n cos(\omega\tau) + B_n sin(\omega\tau). \tag{16}$$

Applying the modified orthogonality relationship (12) together with the initial conditions (6) yields the constants of integration

$$A_n = \int_0^1 V_n(u)g(u)du + \gamma V_n(1)g(1), \tag{17}$$

$$B_n = \frac{1}{\omega_n}\int_0^1 V_n(u)h(u)du + \gamma V_n(1)h(1). \tag{18}$$

3.2 Selection of Modes based on Energy Distribution

The linear superposition of individual modes (14) gives the general solution of the string, but each mode has a distinct influence on the overall behavior of the string. Here, modal participation factors are quantified by adapting the concept of energy distribution among modes of discrete systems (Salsa Jr. and Ma, 2021). In this way, the energy E_n associated with the n-th mode is given by

$$E_n = \frac{1}{2}\int_0^\Gamma [\dot{p}_n(\tau) + \omega_n p_n(\tau)]d\tau, \tag{19}$$

where Γ is the total time of simulation.

The modal selection scheme is as follows. All natural frequencies and mode shapes are computed in a given frequency range $[\omega_1, \omega_2]$. Then, a number N of modes with the highest values of energy are selected and included in the scheme according to

$$v'(u,\tau) = \sum_{n'=1}^{N} V_{n'} p_{n'}(\tau), \tag{20}$$

where $n' = 1$ refers to the most energetic mode while $n' = N$ refers to the less energetic one. These modes form the reduced modal basis of the scheme and, when added to Eq. (20), reflect the approximate solution of the problem. This process is depicted in Fig.2.

3.3 Calculating Errors

The analytic response of the string is important to validate the convergence and evaluate errors of the modal reduction scheme presented herein. However, it requires the evaluation of an infinite sum, which is not possible on a computer. Besides that, truncating the sum is already the objective of the modal reduction methodology. To avoid those issues, a numerical solution of Eq. (5) with a fine mesh will be taken as the true response. The method of lines was used and the space variable was discretized using a second-order finite differences scheme. The spatial variable u was discretized with

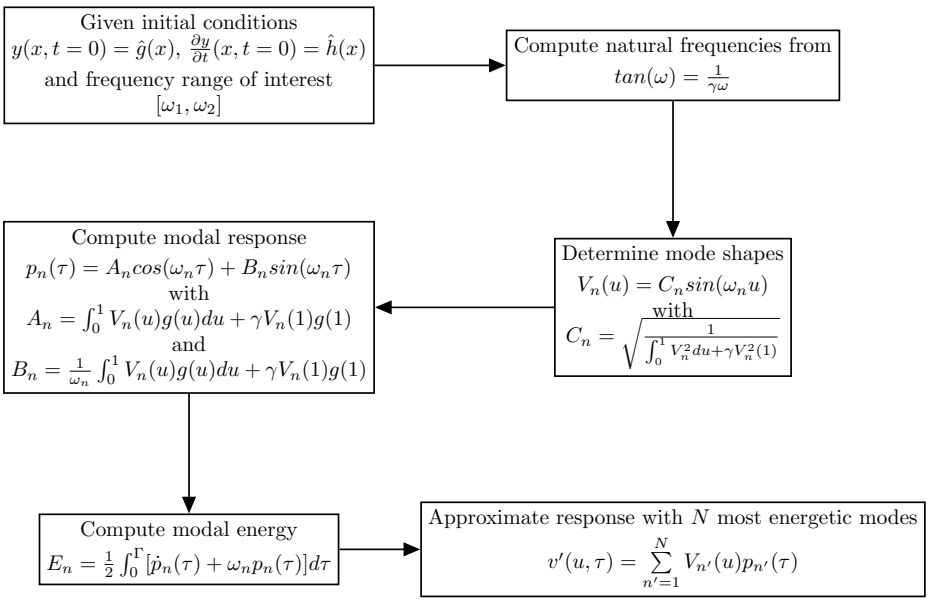

Figure 2. Modal reduction scheme.

$n+1$ points u_j $(j=0,1,2,...,n)$ equally spaced with $h=1/n$. In this approximation, the second-order space derivative is (LeVeque, 2007)

$$\frac{\partial^2 v(u_j,\tau)}{\partial u^2}\approx\frac{v_{j-1}-2v_j+v_{j+1}}{h^2} \tag{21}$$

and the partial differential equation becomes

$$\ddot{v}_j=\frac{v_{j-1}-2v_j+v_{j+1}}{h^2} \tag{22}$$

for the mesh points in the domain: $j=1,2,...,n-1$. The boundary condition at $u=1$ can be approximated by the second-order form

$$2h\frac{\partial v(u_n,\tau)}{\partial u}\approx 3v_n-4v_{n-1}+v_{n-2} \tag{23}$$

to avoid phantom points. Combining Eqs. (22) and (23) with the initial conditions, the problem reduces to solving the system of ordinary differential equations

$$\ddot{v}_1+\frac{2v_1-v_2}{h^2}=0, \tag{24}$$

$$\ddot{v}_j+\frac{-v_{j-1}+2v_jv_{j+1}}{h^2}=0,\quad (2\le j\le n-1), \tag{25}$$

$$2h\gamma\ddot{v}_n+3v_n-4v_{n-1}+v_{n-2}=0. \tag{26}$$

Eqs. (24) - (26) can be cast in the usual matrix-vector form appropriate for computer implementation:

$$,\begin{bmatrix}1&0&\cdots&0\\0&1&&\vdots\\\vdots&&\ddots&\\0&&\cdots&2h\gamma\end{bmatrix}\ddot{\mathbf{v}}+\frac{1}{h^2}\begin{bmatrix}2&-1&\cdots&&&0\\-1&2&-1&&&\vdots\\&\ddots&\ddots&\ddots&&\\\vdots&&\ddots&\ddots&\ddots&\\0&\cdots&&1h^2&-4h^2&3h^2\end{bmatrix}\mathbf{v}=\mathbf{0} \tag{27}$$

where $\mathbf{v}=[v_1\quad v_2\quad\cdots\quad v_n]^T$ is an n-dimensional vector. This system of ODEs can be solved using any appropriate ordinary differential solver with the given set of initial conditions

$$\mathbf{v}(0) = \mathbf{g}, \quad \dot{\mathbf{v}}(0) = \mathbf{h}, \tag{28}$$

where $\mathbf{g} = [g_1 \quad \cdots \quad g_n]^T = [g(u_1) \quad \cdots \quad g(u_n)]^T$ and $\mathbf{h} = [h_1 \quad \cdots \quad h_n]^T = [h(u_1) \quad \cdots \quad h(u_n)]^T$.

The absolute error $|e|$ between the true (numerical) solution and the reduced scheme was calculated at every mesh point, at all instants of time, according with

$$|e|(u, \tau) = |v(u, \tau) - v'(u, \tau)|. \tag{29}$$

The application of the equation resulted in a matrix, $\mathbf{e}_N$, with rows representing the error at equidistant mesh points and columns the error for varying instants of time. The subindex N indicates the number of modes included in the scheme. As the number N increases, is important to better understand how the error varies depending on the influence of each mode on the system.

The root mean square error $RMSE$ was used to provide an alternative measure of error. It was calculated for each time step of the numerical integration

$$RMSE = \sqrt{\frac{1}{\tau}\sum_{i=1}^{\tau}[v(u, i) - v'(u, i)]^2} \tag{30}$$

What was obtained from Eq.(30) is a vector, $\mathbf{r}_N$, which can be represented on a 2-D line plot. These values indicate how much the transversal profile $v'(u)$ diverges from the true one $v(u)$ on the instant i.

4. RESULTS AND DISCUSSION

In this section, the modal reduction scheme is illustrated with three case studies. For illustration purposes, the nondimensional parameter is taken arbitrarily as $\gamma = 1$. The frequency range of interest $[\omega_1, \omega_2] = [0, 100]$ rad/s was chosen.

4.1 Computing Natural Frequencies and Mode Shapes

The natural frequencies can be computed numerically using Newton-Raphson's method. A graphical solution of Eq. (8) is presented in Fig. 3, where each frequency ω_n is visualized by the intersection of the curves $tan(\omega)$ and $1/\gamma\omega$. Thirty-four natural frequencies were found in the given scope and their corresponding modal solutions were calculated.

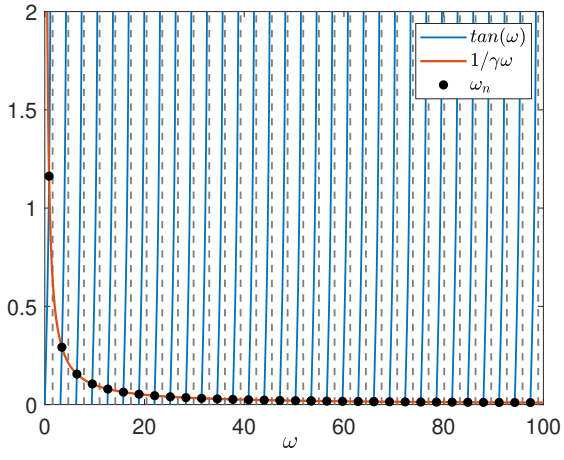

Figure 3. Numerical solution of the frequency equation for a fixed-inertially loaded string. The dashed lines represent the asymptotic behavior of the $tan(\omega)$ function at values multiple of $\pi/2$.

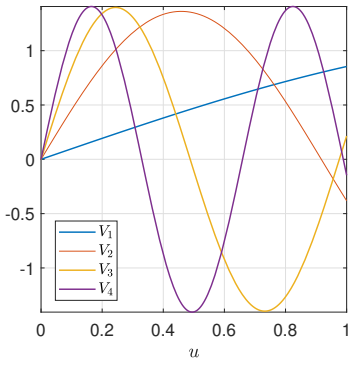

Figure 4. First four modes of a fixed-inertially loaded string.

When vibrating in a given frequency ω_n, the system motion is a stationary waveform associated with the $n-th$ mode. Figure 4 illustrates the first four modal-shape functions of the problem under analysis. These modes represent standing waves where the left boundary is not fixed. In addition, modes 2-4 have nodes while the first mode has none.

4.2 Case 1: Exciting the Second Mode

To validate the methodology, the first case analyzed corresponds to exciting only the second mode of the system. To do that, the initial conditions can be appropriately chosen to mimic the vibration profile of this mode

$$v(u,0) = g(u) = V_2(u), \quad \dot{v}(u,0) = h(u) = 0, \tag{31}$$

from Eqs. (17) and (18): $A_2 = 1$ and $B_2 = 0$. Modified orthogonality relationships shown in Eq. (12) ensure that the effects of the other modes would not be present, $s \neq r \rightarrow \delta_{sr} = 0$. Hence, for any mode in which $n \neq 2$, it is obtained $A_n = B_n = 0$.

Simulation time $\Gamma = 8$ was applied in Eq. (19) to verify the modes with the highest values of energy. Figure 5(a) shows that the modal energy is concentrated in the second mode. In Figure 5(b) notice that considering only the most energetic mode in the reduced scheme ($N = 1$), it is possible to describe the numerical response of the problem.

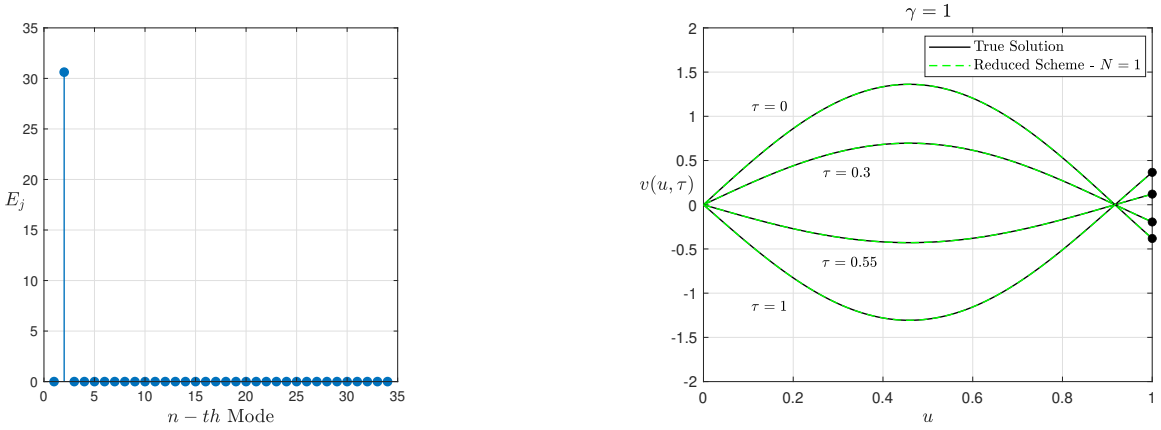

(a) Modal energy distribution. (b) Transverse vibration at different values of τ.

Figure 5. Case study 1, where the initial conditions excite only the second mode.

As expected, when considering the excitation of the second mode only, none of the modes included in the general solution beyond the second one had any impact on the absolute error. This can be observed in Fig. 6, where the representation of the error matrices $\mathbf{e}_1$ and $\mathbf{e}_9$ are practically the same. In other words, the absolute error over the general solution calculation remains unchanged and equal to 0.00055068 independent if other modes are included. These modes have very low energy, but they are still different than zero because of round-off errors.

Figure 6. Representation of absolute error matrices $\mathbf{e}_1$ and $\mathbf{e}_9$. The addition of other modes beyond the second one in the scheme has no influence on the absolute error for the first case studied.

4.3 Case 2: A Linearly Stretched String

The second application involves releasing from rest a linearly stretched string. The initial conditions are

$$v(u,0) = u, \quad \dot{v}(u,0) = 0. \tag{32}$$

Using the same simulation parameters as before, Fig. 7(a) shows that most of the energy is concentrated in the first mode, nevertheless, a small portion of the energy is distributed through the other modes. This happens because the first

mode shape, shown in Fig. 4, has some resemblance to the proposed initial condition (32). This is notable in Fig. 7(b). Despite presenting a very similar transversal profile, it is visible that only the first mode is not sufficient to describe the behavior of the transversal displacement accurately.

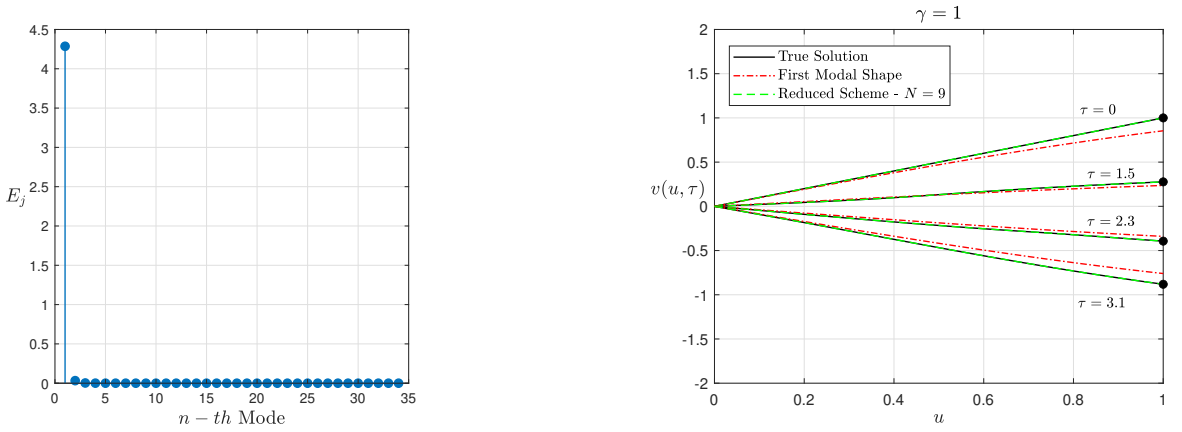

(a) Modal energy distribution.

(b) Transverse vibration at different values of τ.

Figure 7. Case study 2. A Linearly Stretched String.

Accuracy parameters related to case 2 are shown in Fig. 8 and Fig. 9. The error significantly decreases as the modes are added to the scheme, tending to zero. Maximum values of absolute error with $\mathbf{e}_1$ are reduced from 0.0482 to 0.0004736, with $\mathbf{e}_9$, when the nine proposed modes are considered. The same occurs with the representation of the $RMSE$. The plot of $\mathbf{r}_9$ is, in comparison with the other curves, a straight constant line equal to zero.

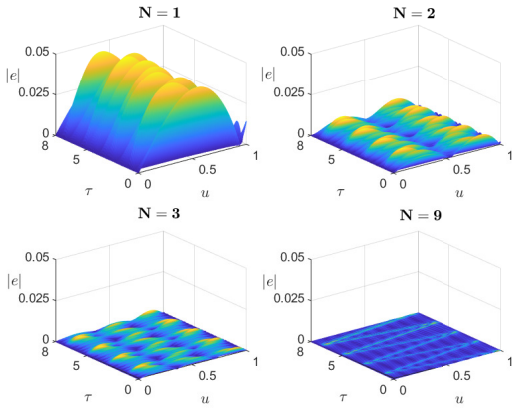

Figure 8. Representation of the absolute error matrices $\mathbf{e}_N$ from case 2.

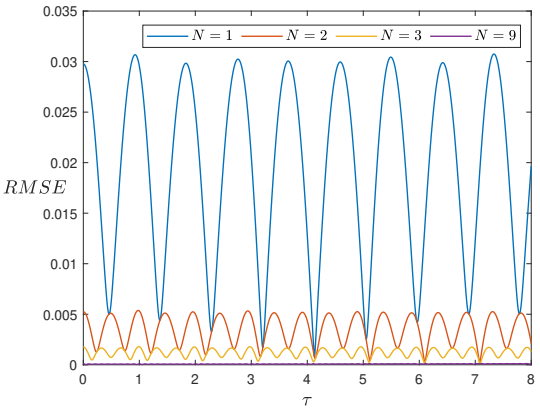

Figure 9. Representation of curves $\mathbf{RMSE}_N$ from case 2.

Those parameters validate the scheme and attest to what is visible in Fig. 7(b). The description of the transversal behavior of the string by the reduced scheme ($N = 9$) and by the numerical solution can be considered the same, taking into account, indeed, the rate of accuracy required for the problem.

4.4 Case 3: A String Plucked at the Middle

Finally, the third application involves releasing a plucked string from rest. In this case, the initial conditions are

$$v(u,0) = \begin{cases} u, & u \leq 0.5 \\ 1-u, & \text{otherwise} \end{cases}, \qquad \dot{v}(u,0) = 0. \tag{33}$$

The modal energy distribution for this case is shown in Fig. 10(a). Here, the energy stored in the modal factors is much more distributed than in the cases analyzed before. Still, a single mode holds the majority of the energy of the problem but is far from accurately representing the transversal displacements of the string, how is shown in Fig. 10(b). Because the string vibrates with normal modes, all points cross the equilibrium position at the same instant.

From Fig. 11 it is important to observe that the maximum levels of absolute error are still very high on the mesh $\mathbf{e}_3$. The precision parameters start to significantly decrease when the fourth mode is accounted for in the scheme ($N = 4$), which is visible in $\mathbf{e}_4$ and in Fig. 12, through $\mathbf{RMSE}_4$.

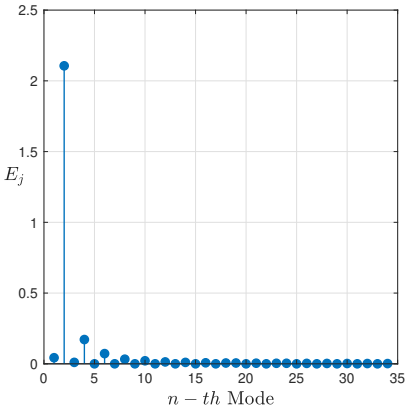

(a) Modal energy distribution.

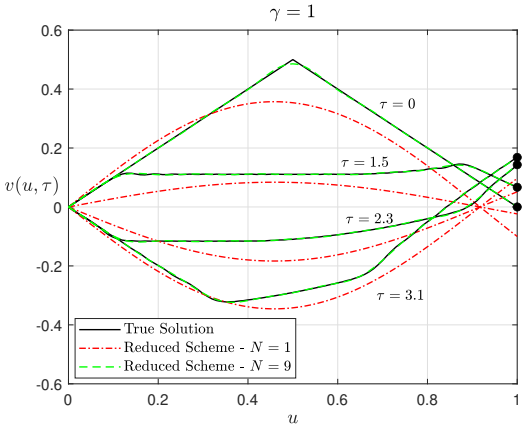

(b) Transverse vibration at different values of τ.

Figure 10. Case study 3. A String Plucked at the Middle.

However, the error parameter decay is not as efficient as the last two examples shown above. Although the transversal profile of the scheme seems noticeably in agreement with the numerical one, as shown in Fig. 10(b), the maximum values for absolute error, 0.0188, in $\mathbf{e}_9$, could not be applicable in the majority of real problems.

That does not represent a limitation to the modal reduced scheme once the number, N, of modes used can be easily extended to reach determined levels of accuracy. In the present paper, N is limited to third-four modes but still, the scheme versatility allows that, according to the given frequency range, this number increases as much as necessary.

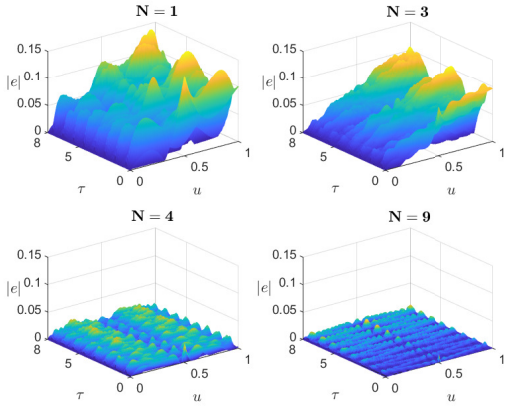

Figure 11. Absolute error represented by the error matrix $\mathbf{e}_N$. Case 3.

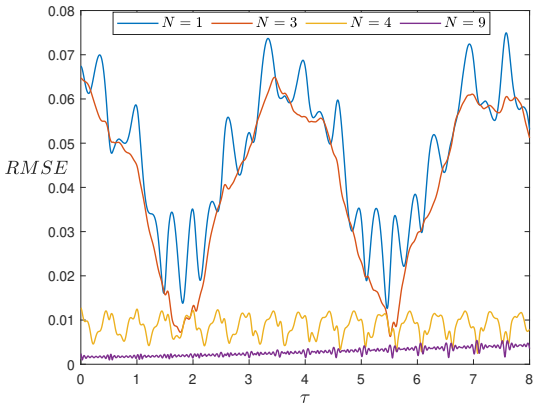

Figure 12. RMSE represented for curves $\mathbf{RMSE}_N$. Case 3.

5. CONCLUSION

This work proposes a modal reduction scheme for a multi-body system, composed of a uniform string fixed at one end and connected to a point mass at the other. The scheme uses a modified orthogonality relationship between the modes to obtain the modal equations. Modal participation factors were estimated using a measure of the energy distribution among modes. The proposed scheme was validated with three different case studies where the errors were measured using an absolute error matrix and a root mean square error. Initially, the 2_{nd} mode of vibration was excited. It was observed that, except for the second mode, no other mode significantly affected the accuracy of the approximation. In the second case study, the system vibrated with more than one mode and the absolute error meshes and $RMSE$ curves showed a substantial decrease as additional modes were incorporated into the scheme. In the final example, the energy distribution was fairly distributed among a few modes. It was observed that considering only the nine most energetic modes of vibration in the reduced scheme might not be sufficient to achieve the same level of accuracy as in the first two examples. However, it is possible to expand the scheme easily to attain a desired level of accuracy while still excluding high-order modes from the solution. The results obtained attest to the flexibility of the scheme in adapting to different scenarios and finding a balance between accuracy and computational efficiency.

6. REFERENCES

Besselink, B., Tabak, U., Lutowska, A., van de Wouw, N., Nijmeijer, H., Rixen, D.J., Hochstenbach, M.E. and Schilders, W.H.A., 2013. "A comparison of model reduction techniques from structural dynamics, numerical mathematics and systems and control". *Journal of Sound and Vibration*, Vol. 332, No. 19, pp. 4403–4422. doi: https://doi.org/10.1016/j.jsv.2013.03.025.

Boggess, A. and Francis, J.N., 2009. *A First Course in Wavelets with Fourier Analysis*. Wiley.

Cox, S.J., Embree, M. and Hokanson, J.M., 2012. "One can hear the composition of a string: Experiments with an inverse eigenvalue problem". *SIAM Review*, Vol. 54, pp. 157–178. doi:10.1137/080731037.

Craig Jr, R.R. and Bampton, M.C.C., 1968. "Coupling of substructures for dynamic analyses." *AIAA journal*, Vol. 6, No. 7, pp. 1313–1319. doi:10.2514/3.4741.

Fehr, J. and Eberhard, P., 2011. "Simulation process of flexible multibody systems with non-modal model order reduction techniques". *Multibody System Dynamics*, Vol. 25, pp. 313–334. doi:10.1007/s11044-010-9238-3.

Genta, G., 2009. *Vibration Dynamics and Control*. Springer.

Gómez, B.J., Repetto, C.E., Stia, C.R. and Welti, R., 2007. "Oscillations of a string with concentrated masses". *European Journal of Physics*, Vol. 28, p. 961. doi:10.1088/0143-0807/28/5/019.

Gómez, B.J., Repetto, C.E., Stia, C.R. and Welti, R., 2009. "Acoustic and quantum-mechanical analogues to the problem of a loaded string fixed at both ends". *European Journal of Physics*, Vol. 30, p. 1107–1117. doi:10.1088/0143-0807/30/5/017.

Hagedorn, P. and DasGupta, A., 2007. *Vibrations and Waves in Continuous Mechanical Systems*. John Wiley Sons Ltd, The Atrium, Southern Gate, Chichester, West Sussex PO19 8SQ, England.

Haller, G. and Ponsioen, S., 2016. "Nonlinear normal modes and spectral submanifolds: existence, uniqueness and use in model reduction". *Nonlinear dynamics*, Vol. 86, pp. 1493–1534. doi:10.1007/s11071-016-2974-z.

Jung, D.W., Han, W., Kim, U.R., Lee, J. and Yu, C., 2021. "Finding normal modes of a loaded string with the method of lagrange multipliers". *Journal of the Korean Physical Society*, Vol. 79, p. 1079–1088. doi:10.1007/s40042-021-00314-9.

LeVeque, R.J., 2007. *Finite Difference Methods for Ordinary and Partial Differential Equations: Steady-State and Time-Dependent Problems*. SIAM, Philadelphia.

Meirovitch, L., 2001. *Fundamentals of Vibrations*. McGraw-Hill.

Mouchet, A., 2008. "Interaction with a field: a simple integrable model with backreaction". *European Journal of Physics*, Vol. 29, p. 1033. doi:10.1088/0143-0807/29/5/015.

O'Reilly, O.M., 2017. *Modelling Nonlinear Problems in the Mechanics of Strings and Rods: the Role of the Balance Laws*. Springer.

Rubin, S., 1975. "Improved component-mode representation for structural dynamic analysis". *AIAA journal*, Vol. 13, No. 8, pp. 995–1006. doi:10.2514/3.60497.

Salsa Jr., R.G. and Ma, F., 2021. *Advances in the Theory of System Decoupling*. Springer.

Sonneville, V., Scapolan, M., Shan, M. and Bauchau, O.A., 2021. "Modal reduction procedures for flexible multibody dynamics". *Multibody System Dynamics*, Vol. 51, p. 377–418. doi:10.1007/s11044-020-09770-w.

Wenin, M., 2022. "Analytical solution of the eigenvalue problem for the elastic cable loaded with a mass point". *Archive of Applied Mechanics*, Vol. 92, pp. 3649–3660. doi:10.1007/s00419-022-02254-7.

7. RESPONSIBILITY NOTICE

The author(s) is (are) solely responsible for the printed material included in this paper.